Optica Applicata, Vol. XLIV, No. 1, 2014
DOI: 10.5277/oa140101

Heterostructure photonic crystal multichannel drop filter based on microcavities and ring resonators

ABDOLLAH AMIRKHANI-SHAHRAKI[1*], MEISAM NIAZI SHAHRAKI[2], MOHAMMAD REZA MOSAVI[1]

[1]Department of Electrical Engineering, Iran University of Science and Technology, Narmak, Teheran 16844-13114, Iran

[2]Department of Electronics Engineering, University of Sistan and Baluchestan, Zahedan, Iran

[*]Corresponding author: abdollah_amirkhani@elec.iust.ac.ir

In this paper, a heterostructure photonic crystal multichannel drop filter based on ring resonators and microcavities is presented. This structure has been made in the form of a two-dimensional square lattice with two regions with refractive indexes of 3.464 and 3.86. The refractive indexes are so chosen as to allow the easy and practical fabrication of the device. The presented heterostructure photonic crystal multichannel drop filter consists of a waveguide, two ring resonators and a microcavity. This microcavity is placed at the end of the bus waveguide. The ring resonators have been installed in two regions with different refractive indexes. These ring resonators act as energy couplers, and at their resonance frequencies, they capture the electromagnetic energy which is transmitted in the bus waveguide. Filter characteristics have been obtained by using the finite difference time domain method. Finally, we will demonstrate that in the optimal structure, at ports B and D (vertical), drop efficiencies close to 90% and 67%, respectively, can be obtained within the third communication window, and at port C (horizontal), an efficiency of almost 80% can be achieved within the second communication window.

Keywords: finite difference time domain method, ring resonators, heterostructure, microcavities, photonic crystal integrated circuits.

1. Introduction

Photonic crystals have alternating structures which do not allow electromagnetic waves with a certain frequency range to pass through them [1]. So by creating a flaw in these types of crystals, light can be considerably confined in this frequency range. This frequency range is known as the photonic band gaps (PBGs). Such unique features

along with the availability of the fabrication technology based on the standard technology of semiconductors have recently brought the photonic crystals to the center of attention. Numerous photonic devices such as lasers, filters and fibers have already been manufactured on the basis of photonic crystals, and for practical applications [2]. One of the most frequently studied subjects is the use of nonlinear light in photonic crystal integrated circuits. In devices that use nonlinear light, the light is controlled by the environment. The need for very high power to produce the nonlinear effects is one of the basic problems afflicting the all-photonic devices that utilize nonlinear light. To eliminate this problem, many solutions have been proposed including the reduction of the device's effective cross-section, the use of materials that have high nonlinear parameters and the use of resonating structures. One of these resonating structures is a ring resonator. In ring resonators, the group velocity diminishes and causes the nonlinear effects to increase. This increase can lead to a reduction in size and the diminishing of nonlinear power threshold.

A high quality factor can increase the nonlinear effects. To obtain a high quality factor in dielectric ring resonators, the ring should be as small as possible. This size reduction in rings can lead to the increase in radiation losses, which makes the dielectric ring resonators inappropriate for use in the all-photonic integrated circuits [3].

Due to having no radiation losses and a flexible design through the tuning of various parameters, the photonic crystal ring resonators are considered as suitable substitutes for the dielectric ring resonators. The parameters that could be adjusted include the radius of scatterer rods, radius of coupling rods and the lattice's dielectric constant [4].

One of the applications of ring resonators is their use in multichannel drop filters. Multichannel drop filters are one of the important components of wavelength multiplexers [5]. These filters can also be used in photonic switches, photonic modulators and dense multiplexers [6].

SHANHUI FAN *et al*. presented the design of channel drop filters based on the square 2-D photonic crystal lattice [7]. The first report on a photonic crystal ring resonator is related to a laser ring in a hexagonal lattice, and it talks about coupling efficiency and the design of modes [8]. ZEXUAN QIANG *et al*. have conducted some studies on add-drop filters based on the square photonic crystal lattice and the use of ring resonators [9]. A multichannel drop filter with three output ports based on ring structures has been presented in [10]. NODA *et al*. investigated the possibility of improving the drop efficiency in heterostructure photonic crystals by using the reflection at the interface [11]. In the most recent studies in [12], a new drop filter based on 2-D triangular photonic crystal lattice with silicone rods has been investigated, and they have achieved an efficiency of over 96% in the direct and reverse drop filters in the third communication window.

In this article, a multichannel drop filter based on a step-by-step design procedure has been presented. This filter has been created by combining two ring resonators, a horizontal waveguide and a microcavity in a 2-D photonic crystal lattice. The reason

for using the microcavity is to reduce the number of waveguide peaks and to improve the efficiency of transmission in the waveguide of vertical drop filter.

2. Calculation of quality factor and the mode coupling theory

Before presenting a general methodology for optimum design, it is better to first find out how quality factor is estimated and how light is coupled in structures such as waveguide, resonator and microcavity according to the mode coupling theory; because we need them in order to describe the operation of the multichannel drop filter. There are two major approaches to calculate the quality factor. In the first approach [13], the following equation is used:

$$Q = \frac{\omega}{\Delta\omega} = \frac{\lambda}{\Delta\lambda} \tag{1}$$

where ω is the angular frequency of resonance, $\Delta\omega$ is the bandwidth, λ is the resonance wavelength and $\Delta\lambda$ is the full width at half maximum (FWHM).

In the second method, since the amplitude of the electric field decreases exponentially, the quality factor can be determined by the following equation:

$$Q = -\frac{\omega_r (T_1 - T_2)\Delta t}{2\ln(E_1/E_2)} \tag{2}$$

where Δt is the time step, and E_1 and E_2 are the electric fields at time steps T_1 and T_2, respectively.

To gain a better understanding of how the presented multichannel filter functions, the Fano mode coupling theory is described. To reduce complexity, a three-port system, with one ring resonator and one microcavity with 100% reflection, is considered.

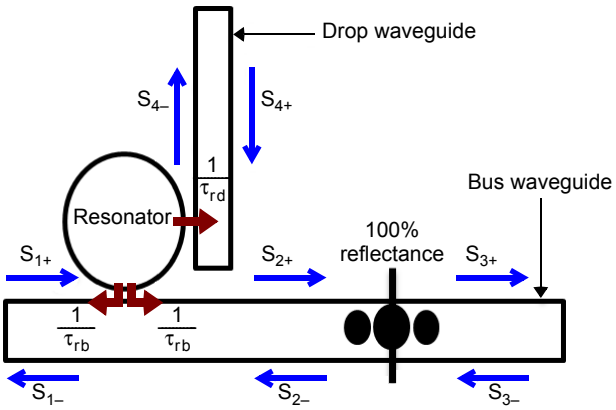

Fig. 1. A schematic of a multichannel filter based on a microcavity with 100% reflection.

The ring resonator in this system is coupled with the bus waveguide from one side and to the drop waveguide from the other side. The theoretical model has been illustrated in Fig. 1. In a Fano resonator, the general dynamic equations for amplitude a of the resonance mode can be written as

$$\frac{\mathrm{d}a}{\mathrm{d}t} = \left(j\omega_0 - \frac{2}{\tau}\right)a + \left(\langle k|^*\right)|S_+\rangle \tag{3}$$

where ω_0 and τ are the central frequency and resonance lifespan, respectively. Amplitude a is normalized in such a way that $|a|^2$ indicates the energy in the resonance mode. Of all the input waves, only one reaches the resonance state and is coupled with the output waves. In the above relation, $\langle k|^*$ is the vector of coupling constants and $|S_+\rangle$ is the vector of input waves, which is shown as

$$|S_+\rangle = \begin{pmatrix} S_{1+} \\ S_{2+} \\ \cdots \\ S_{m+} \end{pmatrix} \tag{4}$$

where m is the number of inputs. Wave reflections can be expressed as follows:

$$|S_-\rangle = C|S_+\rangle + a|d\rangle \tag{5}$$

and $|d\rangle$ denotes the coupling constants and C is the scattering matrix.

When the input wave is at frequency ω, the resonated mode's amplitude is obtained from the following relation:

$$a = \frac{\left(\langle k|^*\right)|S_+\rangle}{j(\omega - \omega_0) + \frac{2}{\tau}} \tag{6}$$

This method is valid only when the width of resonance is much smaller than the resonance frequency. It has been demonstrated in [14–16] that the coupling constants can be considered independent of frequency, and that frequency shifts because the modes decrease exponentially at the ports.

Now in view of Eq. (3), the dynamic equation for amplitude b of the resonated mode in the ring resonator is expressed as follows:

$$\frac{\mathrm{d}b}{\mathrm{d}t} = \left(j\omega_0 - \frac{2}{\tau_{\mathrm{rb}}} - \frac{1}{\tau_{\mathrm{rd}}}\right)b + \sqrt{\frac{2}{\tau_{\mathrm{rb}}}}\left(e^{j\theta_1}S_{1+} + e^{j\theta_2}S_{2-} + e^{j\theta_4}S_{4+}\right) \tag{7}$$

where S_{i+} and S_{i-} are the normalized amplitudes of input and output waves, respectively, and θ_j (j = 1, 2, 3, 4) are the phases of coupling coefficients between the resonator modes and the modes of bus waveguide or drop waveguide. Since we

have a 100% reflection for the microcavity, the amplitudes S_{3+} and S_{3-} would be zero, regardless of the external excitation source. Due to the time-reversal symmetry and power conservation, the relationship between the amplitudes of input and output waves in the waveguides and the resonated mode's amplitude can be expressed as follows.

Assuming $\theta_1 = \theta_2$, we have:

$$S_{1-} = S_{2-} - e^{-j\theta_1}\sqrt{\frac{2}{\tau_{rb}}}\,b \tag{8}$$

$$S_{2+} = S_{1+} - e^{-j\theta_1}\sqrt{\frac{2}{\tau_{rb}}}\,b \tag{9}$$

$$S_{4-} = -S_{4+} + S_{1+} - e^{-j\theta_4}\sqrt{\frac{2}{\tau_{rb}}}\,b \tag{10}$$

Because of the reflection in the microcavity, the amplitudes S_{2+} and S_{2-} are equal, and they only have one phase difference which is due to different distances they travel.

When the input is only launched from the left-side port to the bus waveguide, we get $S_{4+} = 0$

$$\mathrm{Ref}(\omega) = \left|\frac{\overline{S_{1-}}}{\overline{S_{1+}}}\right|^2 = \left|\frac{e^{-j\phi}\left[j(\omega-\omega_0) - \frac{2}{\tau_{rb}} + \frac{1}{\tau_{rd}}\right] - \frac{2}{\tau_{rb}}}{j(\omega-\omega_0) + \frac{2}{\tau_{rb}}(1+e^{-j\phi}) + \frac{1}{\tau_{rd}}}\right|^2 \tag{11}$$

$$\mathrm{Tran}(\omega) = \left|\frac{\overline{S_{4-}}}{\overline{S_{1+}}}\right|^2 = \left|\frac{e^{-j(\theta_4-\theta_1)}(1+e^{-j\phi})\sqrt{\frac{2}{\tau_{rb}}}\sqrt{\frac{2}{\tau_{rd}}}}{j(\omega-\omega_0) + \frac{2}{\tau_{rb}}(1+e^{-j\phi}) + \frac{1}{\tau_{rd}}}\right|^2 \tag{12}$$

where $S_{i\pm}$ are the Fourier transforms of $\overline{S_{i\pm}}$.

It has been stated in [16] that in order to have a 100% transmission, the following relations should be established: $Q_{rb} = 2Q_{rd}$ and $\phi = 2n\pi$.

3. Optimization of the radius of lattice rods

In the first step of optimization, we consider two structures with refractive indexes of 3.464 and 3.86. Since most photonic devices operate within the third communication window, it is necessary to choose such a radius for lattice rods which will make this communication window fall in the middle of the photonic crystal band gap. Moreover, to calculate the photonic crystal band gap in the cascade structures with different refractive indexes, we should calculate the overlapping of the photonic crystal band gaps of all the structures, and consider it as the overall band gap of the photonic crystal

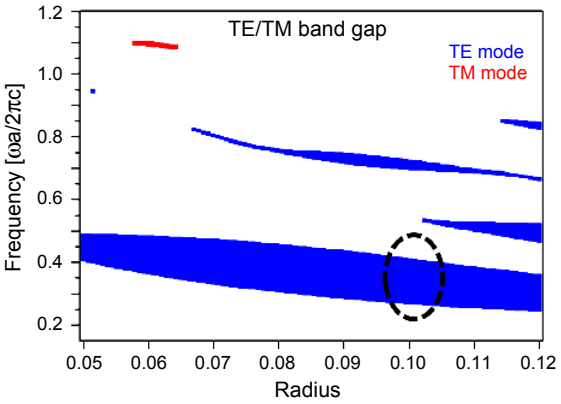

Fig. 2. Photonic crystal band gaps for various radiuses of lattice rods.

structure. The third communication window for the considered structure falls within the range of $0.3323a/\lambda < \delta < 0.3399a/\lambda$. Therefore, it is sufficient to choose a radius at which this interval falls in the middle of the band gap. For this purpose, we calculated photonic crystal band gaps for various radiuses in Fig. 2. As this figure shows, the best radius for the desired objective is $r = 0.1a$, where a is the lattice constant.

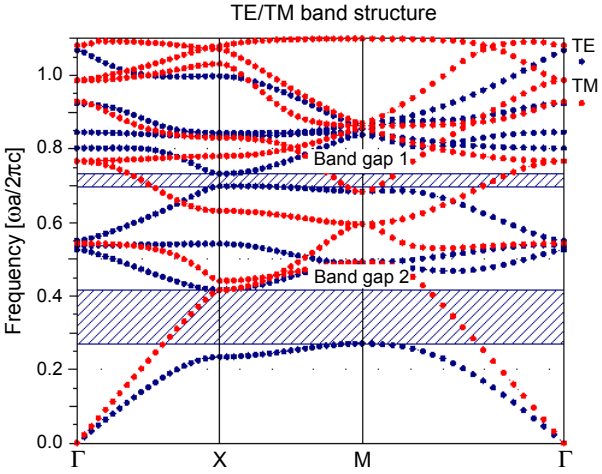

Fig. 3. Scatter diagrams for flawless structure.

Figure 3 illustrates the scatter diagrams for a flawless photonic crystal structure. As can be observed, the structure has two band gaps for the transverse magnetic (TM) mode. Of these two band gaps, band gap 2 is of interest because it falls within the range of communication frequencies. This band gap is in the range of $0.27a/\lambda$ to $0.417a/\lambda$. Lattice constant has been tuned to 520 nm. The general design of the presented structure has been shown in Fig. 4. This structure consists of a waveguide (W1) at the end of which a microcavity is placed. This microcavity has been used to improve the per-

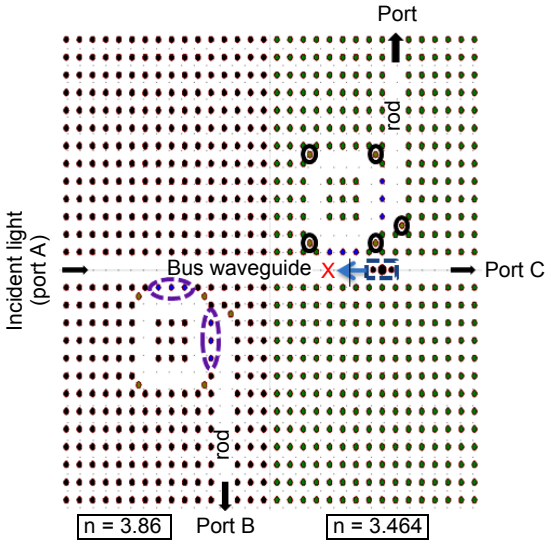

Fig. 4. General structure design of the presented multichannel drop filter based on two ring resonators.

formance of the resonators and to reduce the number of resonance peaks. Also, two ring resonators with odd symmetry about the interface of the two regions have been utilized. The input port, direct transmission port and the drop ports have been labeled as A, B, C and D, respectively. Past works on the design of filters indicate that in order to reduce back scattering and improve the performance of resonators, four rods can be used at four corners of resonators and one rod at the end of the drop filter route. So we also place these rods into each of these resonators. These rods have been marked in the figure by black solid circles. The characteristics of these rods are similar to those of other lattice rods. The blue rods that have been delineated by violet colored ellipses are known as the coupling rods. In this section, a Gaussian light source with a light

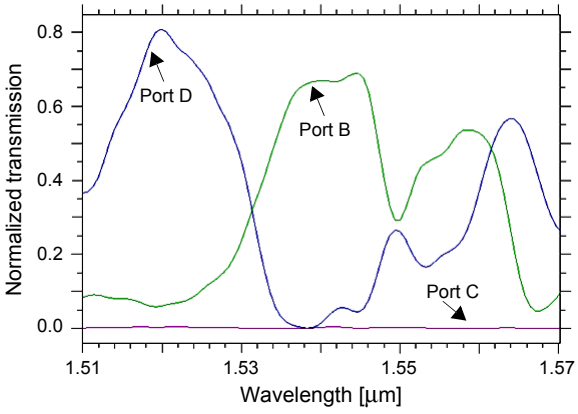

Fig. 5. Normalized transmission diagrams within the communication frequency range at ports B, C and D.

power of unity has been used, which is applied to the input port. Power is monitored at ports B, C and D. Figure 5 shows the normalized transmission diagrams at ports B, C and D. As is observed, ports B and D have transmission efficiencies of about 68% and 80% at frequencies of 1545 and 1521 nm, respectively. Also according to the performed calculations, port C shows a transmission close to zero for this frequency range. Maximum transmission efficiency for this port is close to 30%, which occurs at the frequency of 1310 nm. At this stage, the radius of coupling rods has been considered as $0.089a$. Now, in order to improve the transmission efficiency at each port, we will optimize the radius of coupling rods and change the position of the microcavity. It is also emphasized that during all the design steps, a constant radius, equal to the radius of lattice rods, has been considered for the scatterer rods.

4. Changing the microcavity's position to increase the efficiency

Changing the microcavity's position can be effective in improving the transmission efficiency at port D. So in the following section, we investigate this possibility and evaluate the efficiency for different values of x. As has been shown in Fig. 6, with the position change of x in the indicated direction, the values of efficiency and resonance frequency change. For the three values of $x = 0$, $x = 0.5a$ and $x = 1.0a$, we have monitored the efficiency values at port D. As is demonstrated, the highest transmission efficiency at port D occurs at $x = a$. In this situation, transmission efficiency is equal to 90%, which occurs at the frequency of 1526 nm.

5. Optimization of coupling rods for the increase of efficiency

One of the practices that can help increase the transmission efficiency in ring resonators is the optimization of the coupling rods' radius. In this section, we attempt to find the best radius in order to obtain the highest value of transmission at the ports. For this purpose, we consider the optimum structure of the preceding step (the third structure),

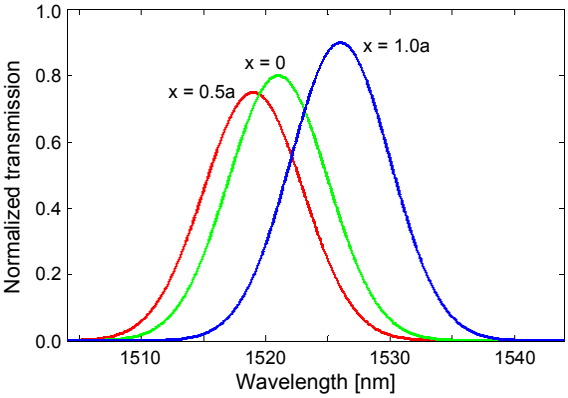

Fig. 6. The effect of changing the microcavity's position on the transmission efficiency of port D.

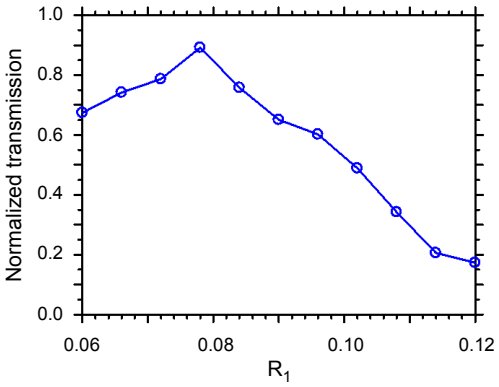

Fig. 7. Transmission efficiency at port B for different radiuses.

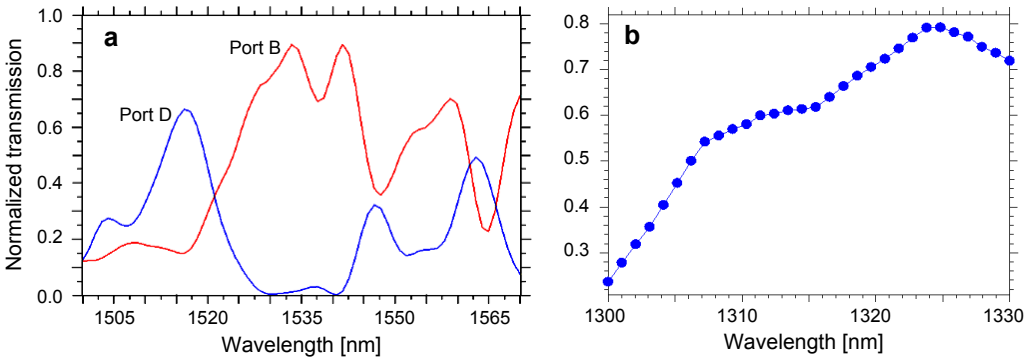

Fig. 8. Normalized transmission at ports B and D in the frequency range of 1500–1570 nm (**a**) and normalized transmission at port C (**b**).

which was obtained at $x = 1.0a$. As is illustrated in Fig. 7, by scanning the radius of coupling rods in the left-side resonator of the third structure for a frequency at which maximum transmission has occurred at this port, we would notice that if we set the radius of the first resonator's coupling rods at $R_1 = 0.078$, the transmission efficiency at ports B and C will increase by about 20% and 10%, respectively. According to Figs. 8**a**, and 8**b**, maximum transmissions at ports B, C and D have occurred at frequencies of 1541, 1325 and 1516 nm, respectively.

T a b l e 1. A comparison between the examined structures.

Number of structure	Transfer in			R_1	R_2	X
	Port B	Port C	Port D			
1	68%	30%	80%	$0.089a$	$0.089a$	0
2	70%	80%	75%	$0.089a$	$0.089a$	$0.5a$
3	70%	70%	90%	$0.089a$	$0.089a$	$1.0a$
4	90%	80%	66%	$0.078a$	$0.089a$	$1.0a$

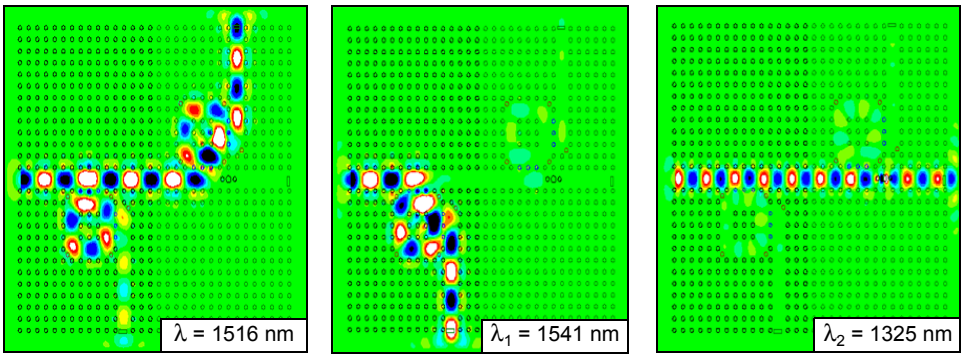

Fig. 9. Electric field pattern.

Efficiency values of transmission in the presented structures for different values of R_1, R_2 and X have been given in Table 1. As is observed, the highest amount of transmission has occurred at port B in the fourth structure, while minimum transmission has taken place at port D in the second structure. From among the proposed structures, the fourth structure is the best. The electric field pattern for the optimum structure has been shown in Fig. 9.

6. Conclusions

In this paper, a heterostructure photonic crystal multichannel drop filter based on ring resonators and a microcavity in a two-dimensional square lattice form was presented. The microcavity used in this structure functions as a 100% reflector at a specific frequency range and enables the considered structure to be used as a device for separating the two main communication wavelengths. The refraction indexes of the structures have been selected so that it would be easy to actually fabricate the device. The design process was carried out via a step-by-step approach, and four different structures were simulated. In the optimum structure, transmission efficiencies of 90%, 80% and 66% were achieved at ports B, C and D, respectively. These structures are of small size and can be used in future photonic integrated circuits.

References

[1] YABLONOVITCH E., *Inhibited spontaneous emission in solid-state physics and electronics*, Physical Review Letters **58**(20), 1987, pp. 2059–2062.

[2] LI L., LIU G.Q., *Photonic crystal ring resonator channel drop filter*, Optik – International Journal for Light and Electron Optics **124**(17), 2013, pp. 2966–2968.

[3] TAMEH T.A., ISFAHANI B.M., GRANPAYEH N., JAVAN A.M., *Improving the performance of all-optical switching based on nonlinear photonic crystal microring resonators*, AEU – International Journal of Electronics and Communications **65**(4), 2011, pp. 281–287.

[4] DJAVID M., ABRISHAMIAN M.S., *Multi-channel drop filters using photonic crystal ring resonators*, Optik – International Journal for Light and Electron Optics **123**(2), 2012, pp. 167–170.

[5] MAHMOUD M.Y., BASSOU G., TAALBI A., *A new optical add-drop filter based on two-dimensional photonic crystal ring resonator*, Optik – International Journal for Light and Electron Optics **124**(17), 2013, pp. 2864–2867.

[6] MONIFI F., FRIEDLEIN J., OZDEMIR S.K., LAN YANG, *A robust and tunable add-drop filter using whispering gallery mode microtoroid resonator*, Journal of Lightwave Technology **30**(21), 2012, pp. 3306–3315.

[7] SHANHUI FAN, VILLENEUVE P., JOANNOPOULOS J., HAUS H., *Channel drop filters in a photonic crystal*, Optics Express **3**(1) 1998, pp. 4–11.

[8] SE-HEON KIM, HAN-YOUL RYU, HONG-GYU PARK, GUK-HYUN KIM, YONG-SEOK CHOI, YONG-HEE LEE, JEONG-SOO KIM, *Two-dimensional photonic crystal hexagonal waveguide ring laser*, Applied Physics Letters **81**(14), 2002, pp. 2499–2501.

[9] ZEXUAN QIANG, WEIDONG ZHOU, SOREF R.A., *Optical add-drop filters based on photonic crystal ring resonators*, Optics Express **15**(4), 2007, pp. 1823–1831.

[10] MONIFI F., GHAFFARI A., DJAVID M., ABRISHAMIAN M.S., *Three output port channel-drop filter based on photonic crystals*, Applied Optics **48**(4), 2009, pp. 804–809.

[11] NODA S.,SONG B. S., AKAHANE Y., ASANO T., *In-plane hetero photonic crystals*, Technical Digest of International Symposium on Photonic and Electronic Crystal Structures V, Kyoto, Japan, 2004.

[12] WEI CHANG WONG, CHI CHIU CHAN, HUAPING GONG, KAM CHEW LEONG, *Mach–Zehnder photonic crystal interferometer in cavity ring-down loop for curvature measurement*, IEEE Photonics Technology Letters **23**(12), 2011, pp. 795–797.

[13] SHIH-CHIEH CHENG, JUN-ZHI WANG, LIEN-WEN CHEN, CHING-CHENG WANG, *Multichannel wavelength division multiplexing system based on silicon rods of periodic lattice constant of hetero photonic crystal units*, Optik – International Journal for Light and Electron Optics **123**(21), 2012, pp. 1928–1933.

[14] SHANHUI FAN, WONJOO SUH, JOANNOPOULOS J.D., *Temporal coupled-mode theory for the Fano resonance in optical resonators*, Journal of the Optical Society of America A **20**(3), 2003, pp. 569–572.

[15] HAUS H.A., *Waves and Fields in Optoelectronics*, Prentice-Hall, Englewood Cliffs, N.J., 1984.

[16] FASIHI K., MOHAMMADNEJAD S., *Highly efficient channel-drop filter with a coupled cavity-based wavelength-selective reflection feedback*, Optics Express **17**(11), 2009, pp. 8983–8997.

Received January 1, 2013